



Coordinated Control of Flexible AC Transmission System Devices and Power System Stabilizer for improve the Power System Stability Using Fuzzy Adaptive Bacterial Foraging

Bahram Khorram¹ and Hamid Lesani²

¹Department of Electrical Engineering, South Tehran Branch, Islamic Azad University, Tehran, Iran,

²Department of Electrical and Computer Engineering, University of Tehran, Tehran, Iran,
b_khorram@yahoo.com, lesani@ut.ac.ir

Abstract: Due to the development of power networks and the ever increasing use of Flexible AC Transmission Systems (FACTS) instruments, the unpredicted interactions have been increased in the power system. Thus, the designing and setting of proper controllers is crucial for the improvement of the dynamic response of a power system along with the FACTS instruments. Because of that in this paper, a new optimization algorithm-based method of Fuzzy Adaptive Bacterial Foraging (FABF) has been used to design the Power System Stabilizer (PSS) and the Thyristor Controlled Series Capacitor (TCSC) for damping the low frequency oscillations of the power system. The aim of this design is to minimize the deviation of speed and generators terminal voltage in a great range of loads with the use of FABF algorithm. Designing of TCSC and PSS has been both independently and simultaneously performed to confirm the discussed method. The comparison of this method with the Particle Swarm Optimization algorithm (PSO) in the 4-machine Kundur system and the 10-machine New England system, shows the superiority potential of this method.

Keywords: Inter-area oscillations, Power system, TCSC, PSS, Coordinated control

1. Introduction

With the advent of large power systems and connecting them, low frequency oscillations in the power system can be seen in the range of 0.3-3 Hz. These oscillations can be damped or remain in the system after appearing, which in that case their amplitude is expanded and causes the fragmentation and instability of the power system [1-2]. Therefore it is necessary for the system to maintain its stability and synchronism when encountering these changes that are known as disturbances. Hence, in the recent decades, different methods have been considered for the designing of power system stabilizer. In the papers, for the designing of power system stabilizers some common methods such as the following ones have been used: phase compensation, poles placement, residual compensation, sensitivity analysis and modern control methods [3]. The problems of these methods include high volumes of calculation, low convergence speed and the possibility of stopping in the local minimum which makes the obtained response not to be optimum. Recently, in order to reduce the design problems in the classic methods, intelligent methods are widely used in the power system stabilizers. For example, the H_∞ method is used to achieve stability and performance characteristic such as reference input permanent state tracing, reduction of the disturbance effect on the performance of the closed-loop system, determination of control signal limitations, and reduction of overshoot [4-5].

But PSSs are designed for the damping of local modes and don't have enough damping ability in the large power systems, especially in the heavy loading conditions in the long transmission lines. In this regard, recent advances in the power electronic industry have led to the utilization of instruments related to FACTS. But considering that both the PSS equipment and FACTS instruments are considered control instruments with quick response, simultaneous utilization of both of them in the power system due to the existence of interaction ability between them, may be destructive to the power system performance. Hence in the recent years,

Received: June 30th, 2014. Accepted: June 19th, 2015

in order to reduce the existing interactions and to promote the performance level of the power systems, the researchers' approach has been directed towards the simultaneous design of FACTS and PSS controllers instruments, some of which to be mentioned are: Static VAR Compensator (SVC), Static Synchronous Series Compensator (SSSC), Static Synchronous Compensator (STATCOM), etc [6-9]. In this paper, simultaneous control of PSS and another product of the FACTS family that is TCSC, have been taken into consideration. Thyristor controlled series compensator (TCSC) as one of the FACTS controllers is used to increase the stability and damping of the oscillations in the power systems [10-12]. TCSC can take up different roles in the power system some of which to be mentioned are: power system damping, increasing the transmission capacity from the line, transient stability improvement, fault current limiter and sub-synchronous resonance damping [13].

In the recent years, the examination of TCSC control methods have caught the attention of many researchers to the extent that different control methods have been introduced for the control of TCSC, some of them to be mentioned are pole placement [14], robust control [15], adaptive control [16], intelligent control methods [15-18-20] and nonlinear control [21-22]. In [15] with the use of design method in time domain, robust controller has been offered for the damping of the power system oscillation, and the results taken from robust controller simulation have been compared with the results taken from phase lead-lag controller. In [16] the designed damper controller is adaptive and the parameters of the power system are estimated according to a simple genetic and power system model. Also in [17] neural controller, in [18] self-adjusting proportional-integral fuzzy controller has been offered. In [19] back-propagation based fuzzy PID adaptive controller was designed. In this type of design, controller parameters are dynamically adjusted by neural network output. In [21] model-based nonlinear controller and in [22-23] also non-linear controller have been designed using the Lyapunov function. In [24] for the purpose of pole placement for PSS and TCSC, gradual cooling algorithm of SA has been used. In [25] with the use of particle swarm algorithm, the coordinated design of PSS and TCSC has been mentioned. In this research a new powerful method called FABF algorithm [26] has been used for the optimum design of the proposed controlling parameters with the aim of reducing the existing interaction in the power system and with the consideration of varied exploiting conditions. Also to ensure the resistance of the controller designed by this method, the system performance has also been examined under an intense disturbance. Evaluation of the results taken from the simulation carried out in the time domain, confirms the suitability of the proposed model for TCSC and effective damping efficiency of the controller designed by the FABF method, in the improvement of power system stability. Also the results clearly show the superiority of the coordinated design of PSS and TCSC compared to the separate design of each of these instruments. This superiority has been demonstrated in the ITAE framework of performance indicator.

2. Introduction of the Algorithm

Vestiges of the living types in every revolutionary process depend on their own measures of fitness which is dependent on foraging and animal behavior. Law of evolution supports the ability of better foraging and or removing or reshaping of them with poor foraging ability. The stronger genes, in the evolutionary chain in the future generations reproduce to the types that have better breeding ability. Therefore, clear understanding of the foraging modelling of each of the evolutionary types, has brought about the proper application in nonlinear system optimization algorithm. Foraging strategy of the E.coli bacteria in the human intestine can be explained through the four processes written below:

1. Chemotaxis
2. Swarming
3. Reproduction
4. Elimination & Dispersal

A. Chemotaxis

The movement characteristics of the bacteria in foraging can be defined in the two forms of swimming and tumbling, which combined together are known as Chemotaxis. If bacteria is moving in a pre-defined path, it would be called "is swimming" and if it moves in a totally different direction then it would be called "is tumbling". Mathematically, the tumbling of every bacterium can be shown by a random longitudinal unit of the path (i), which is multiplied by the length of the step of the bacterium $C(i)$. If swimming, this random length would be pre-defined.

In order to reach the optimum value of the step in a shorter time, a domain exists in fuzzify for the $C(i)$ variable. At the beginning of the move, the $C(i)$ vector value is randomly selected and this selection plays an important role in the convergence of the SBF algorithm [24]. The small value of $C(i)$ causes the reduction of convergence, and the large values may, by setting the minimum of swimming, continuously divert the bacteria. Thus, selection of $C(i)$ in SBF is sensitive, time taking and exhausting. Hence, to ensure the convergence of the SBF algorithm, the fuzzy adaptation method has been used to determine $C(i)$ [28]. In this method, the fuzzy input variables are considered as $C(i)$ and the error of target function, gives the fuzzy output as the optimum value of $C(i)$. For the $C(i)$ movement vector step, the fuzzy toolbox in MATLAB 7.6 software, utilized fuzzify.

B. Swarming

In the process of reaching to the richest source of forage for the bacterium (e.g. for the algorithm for the convergence in a more proper point), it is important for the bacterium to try to absorb another bacterium during the desired periods of foraging, so that they will quickly become convergent in the targeted point. To achieve this, a penalty function based on the relative distance of each bacterium from a more proper bacterium to that time of foraging is added to the original cost function. Finally, when all the bacteria are integrated together in the desired point, this penalty function becomes zero. The effect of swimming is for creating bacteria swarms for the groups and the movement is in the form of concentric pattern with large swarms of bacteria.

C. Reproduction

The main collections of the bacteria get evolved after taking several chemotactic levels, and reach the stage of reproduction. Here, the best collection of bacteria is divided into two groups. The healthier half replaces the other half of the removed bacteria, and this action will make the population of the bacteria to remain unchanged during the process of evolution.

D. Elimination and Dispersal

It is possible that in the local environment, the life of a population of bacteria changes either gradually by consumption of nutrients or suddenly due to some other influence. Events can kill or disperse all the bacteria in a region. They have the effect of possibly destroying the chemotactic progress, but in contrast, they also assist it, since dispersal may place bacteria near good food sources. Elimination and dispersal helps in reducing the behavior of stagnation (i.e., being trapped in a premature solution point or local optima).

The flow chart of the proposed FABF algorithm is shown in Figure 1.

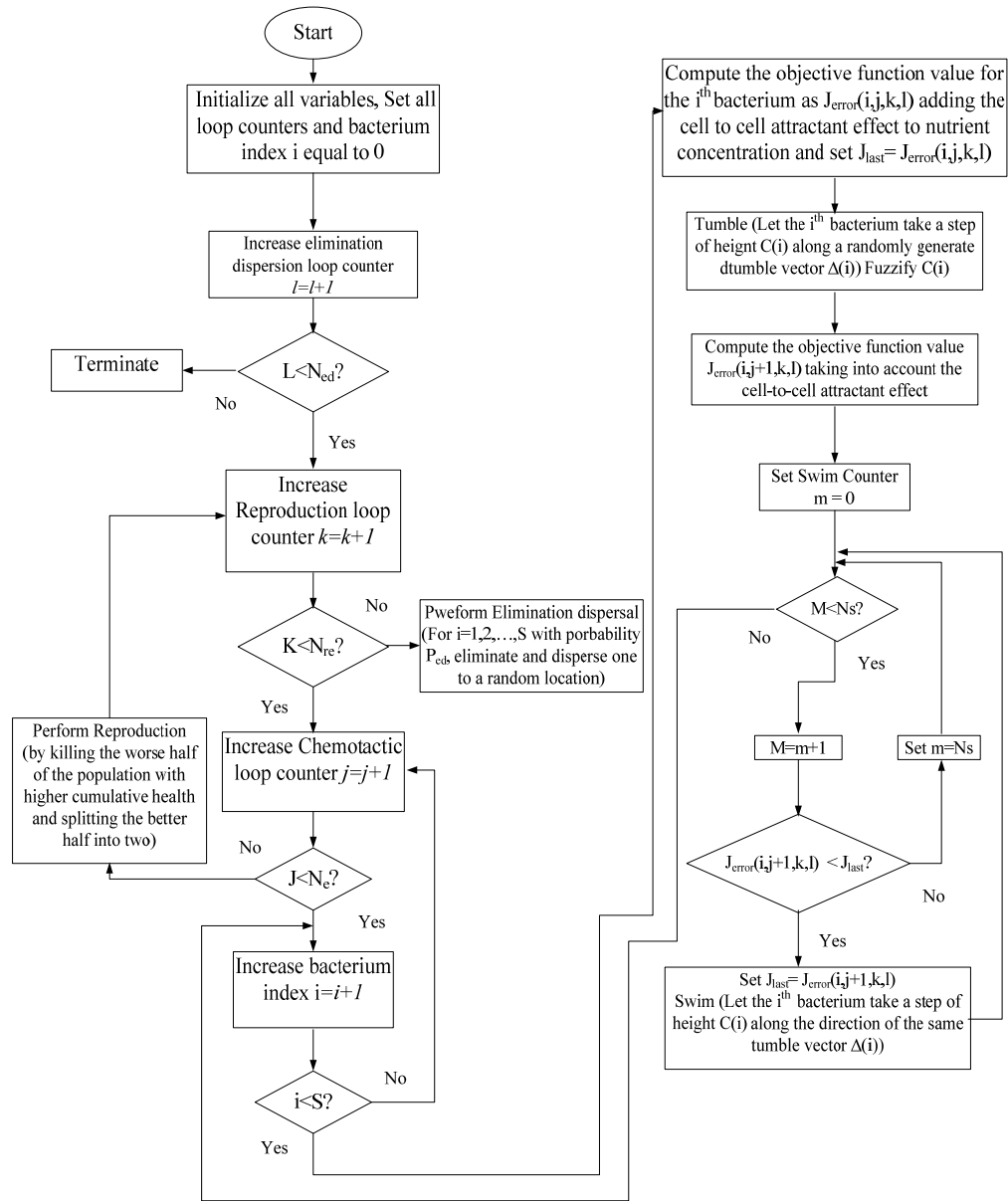


Figure 1. Flowchart of fuzzy adaptive bacterial foraging algorithm

The FABF algorithm proposes the optimum design of the PSS and TCSC controllers in the multi-machine power system in an independent and also a coordinated way. The coding of the proposed FABF algorithm for the management of rescheduling of the PSS and TCSC controllers optimization in the multi-machine power system is as follows:

1. Initialize parameters p , S , N_s , N_e , N_{re} , N_{ed} , P_{cd} , $C(i)$ ($i = 1, 2, \dots, S$), θ^i .
2. Elimination-dispersal loop: $l = l + 1$
3. Reproduction loop: $k = k + 1$
4. Chemotaxis loop: $j = j + 1$
 - [a] For $i = 1, 2, \dots, S$ //take a chemotaxis step for bacterium i

[b] Compute fitness function $J_{\text{error}}(i,j,k,l)$.

$$J_{\text{error}}(i,j,k,l) = J_{\text{error}}(i,j,k,l) + J_{\text{cc}}(\theta^i(j,k,l), P(j,k,l))$$

[c] $J_{\text{last}} = J_{\text{error}}(i,j,k,l)$ //to save this value to find a better cost

[d] Tumble:

Generate a random vector $\Delta(i) \in \mathbb{R}^p$ with each element $\Delta_m(i)$, where $m = 1, 2, \dots, p$, a random number on $[-1, 1]$.

[e] Move:

$$\theta^i(j+1, k, l) = \theta^i(j, k, l) + C(i) \Delta(i) / \sqrt{\Delta^T(i) \Delta(i)} \quad (1) \text{ //step size } C(i) \text{ for bacterium } i.$$

Fuzzify the variable $C(i)$

[f] Compute $J_{\text{error}}(i,j+1,k,l)$

$$J_{\text{error}}(i,j+1,k,l) = J_{\text{error}}(i,j+1,k,l) =$$

$$J_{\text{error}}(i,j+1,k,l) + J_{\text{cc}}(\theta^i(j+1,k,l), P(j+1,k,l)) \quad (1)[g] \text{ Swim } m = 0$$

//counter for swim length While $m < N_s$

$m = m + 1$

If $J_{\text{error}}(i,j+1,k,l) < J_{\text{last}}$ //if doing better

$$J_{\text{last}} = J_{\text{error}}(i,j+1,k,l)$$

$$\theta^i(j+1, k, l) = \theta^i(j+1, k, l) + C(i) \Delta(i) / \sqrt{\Delta^T(i) \Delta(i)} \quad (3) J_{\text{error}}(i,j+1,k,l) = J_{\text{error}}(i,j+1,k,l) + J_{\text{cc}}(\theta^i(j+1,k,l), P(j+1,k,l))$$

4. Else, $m = N_s$ //End of while statement

[h] Go to next bacterium $(i+1)$ if $i \neq S$ //Go to process the next bacterium

5. If $j < N_c$, Go to 4 //to continue chemotaxis, since the life of the bacteria is not over

6. Reproduction:

For the given k and l , and for each $i = 1, 2, \dots, S, N_c+1$

$$J_{\text{health}}^i = \sum_{j=1}^{N_c+1} J_{\text{error}} \quad (5) \text{ If } k < N_{\text{re}}, \text{ Go to 3 //to perform}$$

reproduction

7. Eliminationdispersal:

For $i = 1, 2, \dots, S$, with probability p_{ed} ,

Perform elimination dispersal //to eliminate and disperse one to a random location

If $l < N_{\text{ed}}$, Go to 2 Otherwise end.

3. Power system modelling

A. Synchronous generator and power system stabilizer

Consider a power system with n number of generators in which the dynamic model of the i (th) machine based upon the 5 ordinary differential equations, has been shown in the equations (1) to (5) [29].

$$\frac{d\delta_i}{dt} = \omega_o \omega_i \quad (1)$$

$$\frac{d\omega_i}{dt} = -\frac{1}{2H_i} [P_{mi} - P_{ei} - D_i \omega_i] \quad (2)$$

$$\frac{de'_{di}}{dt} = [-e'_{di} - (x_{qi} - x'_{di}) I_{qi}] \frac{1}{T'_{qoi}} \quad (3)$$

$$\frac{de'_{qi}}{dt} = [E_{fdi} - e'_{qi} - (x_{di} - x'_{di}) I_{di}] \frac{1}{T'_{doi}} \quad (4)$$

$$\frac{dE_{fd}}{dt} = -\frac{1}{T_{Ai}} (E_{fdi} - E_{fdi0}) - \frac{K_{Ai}}{T_{Ai}} (V_{ti} - V_{ti0}) \quad (5)$$

Which δ , ω , H , P_m , P_e , D , e'_d , e'_q , x_d , x'_d , I_d , E_{fd} , T'_{do} , K_A , T_A , V_t are angle, angular velocity of the rotor, inertia constant, mechanical input power, electric output power, damping coefficient, internal voltage of the d and q axes, synchronous reactance and transient of d and q axis, axial flow of d and q armature, excitation voltage, d axis transient time constant, gain and time constant of excitation, and synchronous generator terminal voltage, respectively.

Axial flow of d and q armature of synchronous generator is obtained as follows:

$$I_{di} = \sum_{j=1}^n e'_{qi} (G_{ij} \sin \delta_{ij} - B_{ij} \cos \delta_{ij}) \quad (6)$$

$$I_{qi} = \sum_{j=1}^n e'_{di} (B_{ij} \sin \delta_{ij} - G_{ij} \cos \delta_{ij}) \quad (7)$$

Which G_{ij} and B_{ij} : are real and imaginary part of the (i,j) admittance matrix element.

The classic power system stabilizer has phase-lag structure which has been shown in Figure 2 and the excitation is of D-type1.

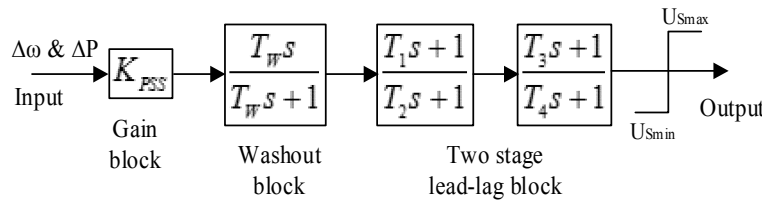


Figure 2. Lead-lag structure of power system stabilizer

B. TCSC modelling and damping controller design

TCSC circuit model with its control block diagram is shown in Figure 3. TCSC has three main parts: C capacitor, L bypass inductor and bidirectional thyristors. The firing angle of thyristors are controlled in a way so that the TCSC reactance would be adjusted according to the control system algorithm, and usually the (α) firing angle would be readjusted due to the created changes in system parameters. According to Figure3 it can be seen that by changing the switching of bidirectional thyristors, the TCSC reactance can be an inductive or capacitive variable. Therefore, according to capacitor voltage, Thyristor Controlled Reactor (TCR), is fired by thyristors phase angle in the angular range of 90 to 180 degrees. It's possible to model TCSC as the variable reactance for the power flow studies and dynamic stability analysis.

The dynamic equation of TCSC reactance can be defined as follows:

$$\Delta \dot{X}_{TCSC} = \frac{1}{T_s} (K_s (\Delta X_{TCSC}^{ref} + \Delta U_{TCSC}) - \Delta X_{TCSC}) \quad (8)$$

In the X_{TCSC}^{ref} equation (8) of TCSC reference reactance, K_s , T_s are gain and time of TCSC. As can be seen from section (b) of Figure 3, TCSC block diagram includes these three parts: gain block, signal washout block, and phase lead-lag.

It's necessary to mention that since FACTS instruments are used in transmission systems, when choosing input signals, local signals are always preferred over broad signals. Hence, the input signal in the given multi machine system, is considered as the speed and voltage variation between two areas.

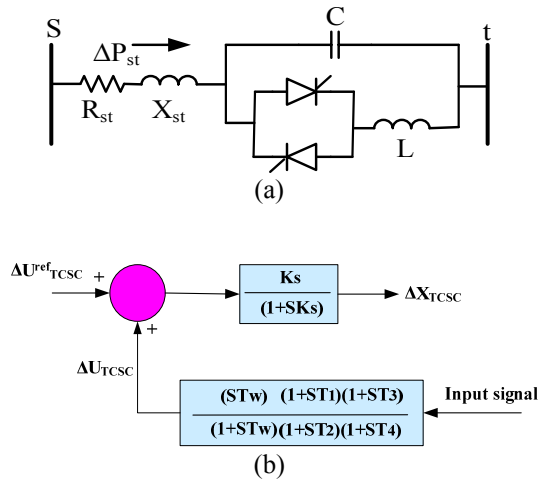


Figure 3. Makeup of TCSC included: (a) Circuit model of TCSC
(b) Diagram block of TCSC controller

C. Damping controller design for the multi-machine power system

In order to improve the damping of power system oscillation, the duty of damping controller is to produce electrical torque in-phase with controller input signal. In this regard, in order to maintain stability and reduce low frequency oscillation, the coefficients of TCSC and PSS controllers can be identified using ranges shown in Figure 4 for the determined target function in equation (9).

$$ITAE = 1000 \int_0^{t_{sim}} t \left(\sum_{i=1}^4 \sum_{j=1}^4 |\Delta \omega_{i,j}| + \sum_{i=1}^4 |\Delta V_{ti}| \right) dt, i \neq j \quad (9)$$

Which, t_{sim} of simulation time, ΔV_{ti} of voltage deviation, i_{th} of generator, and $\Delta \omega_{i,j}$ are oscillations between of the two generators.

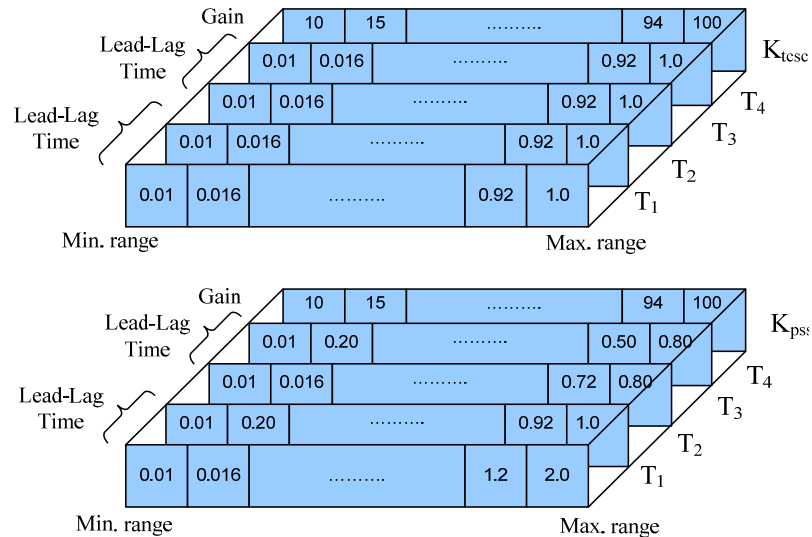


Figure 4. Particle configurations (A) TCSC control and (B) PSSs controllers

In order to design PSS and TCSC controller for every area of the power system shown in Figure 5, one of the PSSs (PSS1, PSS3) was considered for the simultaneous design with TCSC which is installed between the buses 8 and 9. Parameters of the proposed controllers are designed using FABF method. In this case, due to this combination of the parameters, the controllers will have the best performance, and the damping of the oscillations will reach its best status. Damping controller of Figure (2) and (3) with speed variations signals ($\Delta\omega$) and voltage variations (ΔV) of two areas as input, should be able to produce enough damping torque for the improvement of the stability conditions of under-testing multi-machine power systems in Figure (5) and (6). For this purpose and also for the optimization of the performed design, phase lead-lag dynamic compensator parameters, $K, T1, T2, T3$ and $T4$, under operational conditions in table 2 and with the goal of the minimization of the fitness function value (ITAE) defined in equation (9), were determined using the FABF algorithm.

Table 2. Loading conditions for the system (in p.u.).

| Generator | Light | | Normal | | Heavy | |
|-----------|--------|--------|--------|--------|--------|--------|
| | P | Q | P | Q | P | Q |
| G_1 | 0.7323 | 0.1711 | 0.7767 | 0.1524 | 0.8268 | 0.1297 |
| G_2 | 0.7183 | 0.1888 | 0.7659 | 0.1799 | 0.8199 | 0.1689 |
| G_3 | 0.7679 | 0.1337 | 0.8163 | 0.1090 | 0.8712 | 0.0793 |
| G_4 | 0.7404 | 0.1266 | 0.7912 | 0.1119 | 0.8492 | 0.0936 |

This design has been done for the TCSC and PSSs controller, by considering the constraints shown in Figure 4.

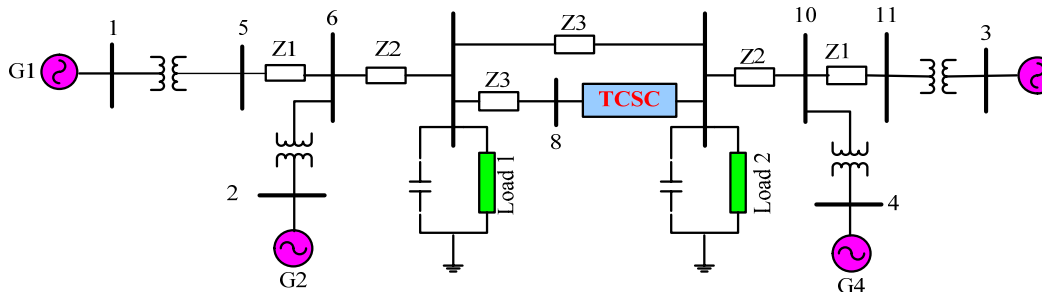


Figure 5. 4-Machine power system with the TCSC

The 4-machine power system shown in Figure 5 consists of two symmetrical areas which are connected together by two 230 kV transmission lines with the length of 220km. Also in every area, two synchronous generators with the nominal power of 20kV/900MVA have been used [3]. The second power system which is shown in Figure (6), is the New England 10 machine power network, and the information related to this system including, generators dynamic equations, excitation system and PSSs are given in [30]. According to Figure (6), the Single-line diagram of this system includes 10 generators, 39 buses and 46 transmission lines. This system can be considered as an infinite-bus connected single-machine (10th generator) system. From the perspective of inter-area low frequency oscillation, some lines are a proper place for TCSC installation. In this regard, the position of TCSC placement is between the buses 1 and 2 and also buses 8 and 9 [31].

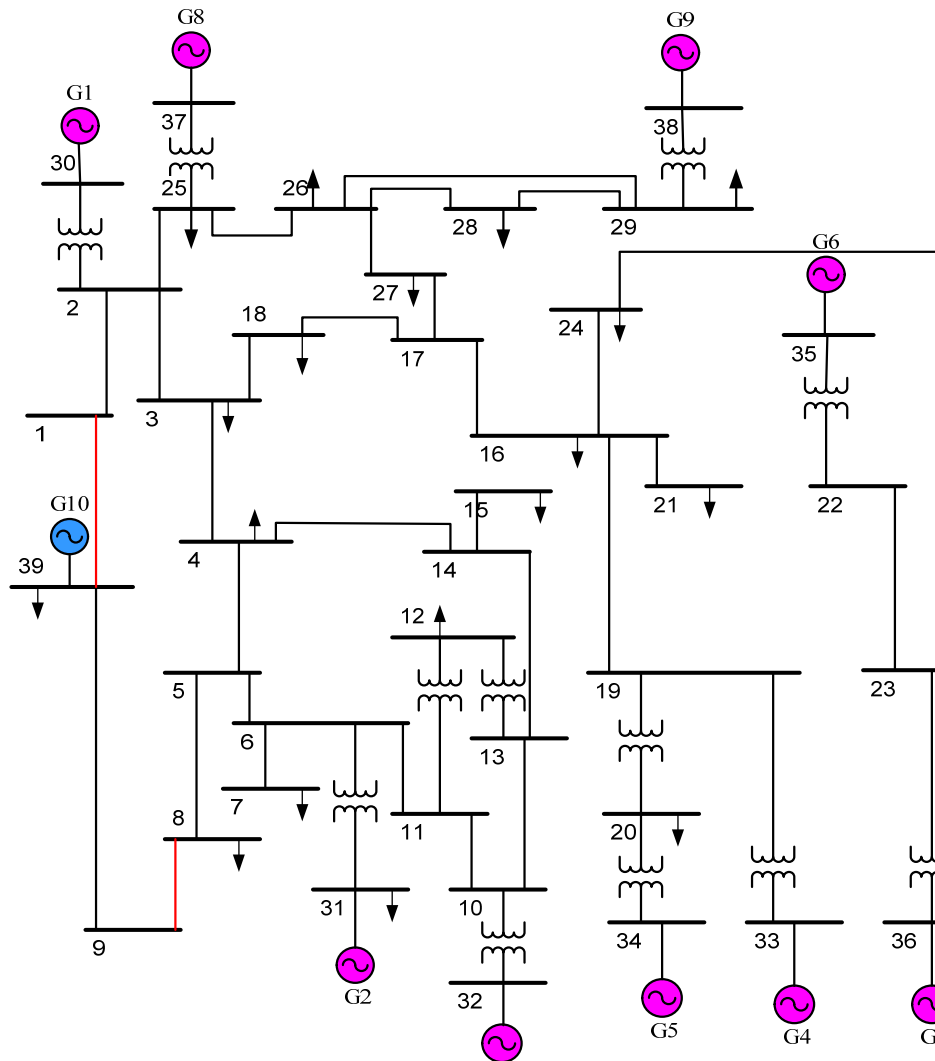


Figure 6. Single line diagram of NEIPS

5. Simulation results

A. The 4-machine power system simulation results

In this paper, the performance of the FABF proposed method on the 4-machine and 10-machine system, has been considered as an optimization issue for the purpose of power system stability and reduction of the existing interaction between TCSC and PSS. Optimization parameters by FABF algorithm which includes the TCSC and PSSs controller coefficients, have been provided in table 2. Also in table 3, special values of local and inter-area modes resulted from different designs of PSSs and TCSC controllers, have been shown for the 4-machine system under nominal loading condition by the given method of FABF. Also, as can be seen, the existence of unstable inter-area mode while the controller isn't being used, is in the location of $0.1082 \pm i4.027$. But despite the coordinated controller design of TCSC, PSS1 and PSS3, this unstable inter-area mode has been transmitted to the $-2.13 \pm i3.52$ with the damping ratio of 0.517, which shows the power system stability.

Table 2. The optimal parameter settings of the proposed controllers

| Controlle r paramete rs | Coordinated | | | Uncoordinated | | |
|----------------------------------|-------------|------------------|------------------|---------------|------------------|------------------|
| | TCS C | PSS ₁ | PSS ₃ | TCS C | PSS ₁ | PSS ₃ |
| K _p | 25.34 | 36.2 5 | 39.6 5 | 30.23 | 48.32 | 51.1 0 |
| T ₁ | 0.23 | 0.53 | 0.48 | 1.46 | 0.70 | 0.46 |
| T ₂ | 1.12 | 0.41 | 0.50 | 0.87 | 0.26 | 0.17 |
| T ₃ | 0.95 | 1.17 | 1.28 | 0.78 | 0.57 | 0.65 |
| T ₄ | 0.96 | 1.12 | 0.81 | 1.17 | 0.79 | 0.52 |

Table 3. The various modes of oscillation of the closed loop with PSSs and TCSC for two areas 4-machine systems in nominal load conditions

| Type of mode | Without Controller | TCSC Controller | PSS Controller | Uncoordinated PSS & TCSC | Coordinated PSS & TCSC |
|-----------------|---|---|--|--|------------------------------------|
| Inter-area mode | 0.1082± i4.027ξ=- 0.0268 f=0.641 | -0.895 ± i3.938 ξ=+0.257 f=0.627 | -1.051 ± i3.938 ξ=+0.257 f=0.627 | -1.45 ±i4.01 ξ=+0.34 f=0.64 | -2.13 ±i3.52 ξ=+0.517 f=0.56 |
| Local mode 1 | -0.669 ± i7.047 ξ=+0.094 f=1.122 | -0.235 ± i7.02 ξ=+0.033 f=1.118 | -3.021 ± i9.755 ξ=+0.296 f=1.553 | -1.45 ±i12.01 ξ=+0.12 f=1.91 | -2.79 ±i11.82 ξ=+0.23 f=1.87 |
| Local mode 2 | -0.677 ± i7.269 ξ=+0.095 f=1.157 | -0.646 ± i7.272 ξ=+0.088 f=1.158 | -3.023 ± i10.243 ξ=+0.283 f=1.631 | -1.352 ± i10.211 ξ=+0.13 f=1.62 | -2.51 ±i12.33 ξ=+0.20 f=1.94 |

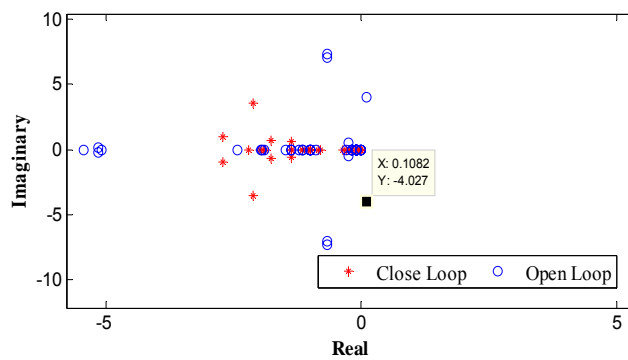


Figure 7. Eigen values of the open loop and closed loop power system with 4-machine

Table 2, adjusted optimized parameters for the proposed controllers. Also, in figure 7, two unstable inter-area modes in the (open-loop) controller-less form of the system, which is shown in $0.1 \pm 4.02i$ points, these two modes are transmitted to the left side of the imaginary axis ($j\omega$), using the proposed algorithm, making the power system stable in the inter-area mode. The effect and power fullness of the proposed controllers' performance are examined under transient conditions in the middle of the transmission line (bus 7 and 8) by applying the three-phase short circuit error at Time=1s for 150 ms. The structure of the power system is maintained at the time of error occurrence and the system recovers back to normal conditions, after the elimination of the error.

B. The nominal loading results in the 4-machine power system

In this section the output results, resulted from speed deviation of generators: $\Delta\omega_{13}$, $\Delta\omega_{34}$, $\Delta\omega_{14}$, by the proposed controllers under nominal loading conditions, were show in figures 8, 9 and 10, respectively. According to these figures, the performance of the proposed controller in the coordination between PSS and TCSC for the reduction of settling time, and thus damping of the power system's oscillations, is clearly observed. In order to further prove the method used in figure 11, the response of $\Delta\omega_{13}$ has been compared using the two different optimization techniques: FBFA and PSO. According to this figure, the amounts of overshoot, under shoot and settling time are 0.61×10^{-3} , 0.72×10^{-3} and 3.78S, respectively. Where as these amounts in designing by the particle swarm algorithm are 0.58×10^{-3} , 1.4×10^{-3} and 5.30, respectively.

The obtained results imply the superiority of FABF algorithm over PSO algorithm.

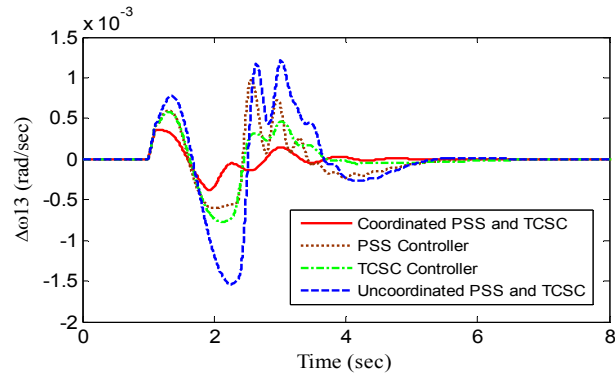


Figure 8. Response of $\Delta\omega_{13}$ for normal load condition

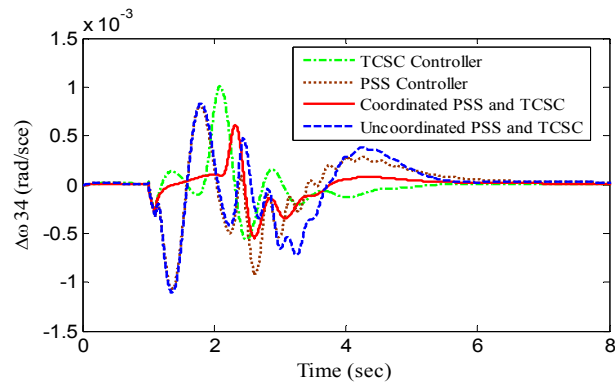


Figure 9. Response of $\Delta\omega_{34}$ for normal load condition

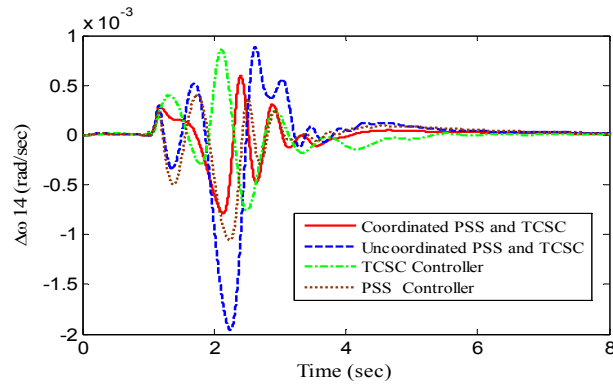


Figure 10. Response of $\Delta\omega_{14}$ for normal load condition

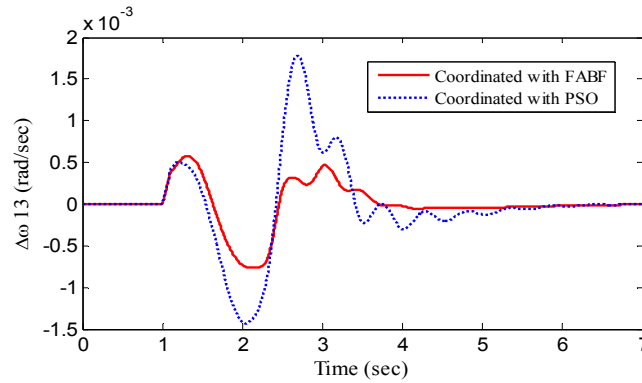


Figure 11. Response of $\Delta\omega_{13}$ for different optimization techniques

C. The light loading response results in the 4-machine power system

In this section the output results, resulted from speed deviation of generators: $\Delta\omega_{13}$, $\Delta\omega_{34}$ and $\Delta\omega_{14}$ by the proposed controllers under nominal loading conditions were show in figures 12, 13 and 14, respectively. According to these figures, the performance of the proposed controller in the coordination between PSS and TCSC for the reduction of settling time, and thus the damping of the power system's oscillations, is clearly observed. In order to further prove the method used in figure 15, the response of $\Delta\omega_{13}$ has been compared using the two different optimization techniques: FBFA and PSO. According to this figure, the amounts of overshoot, under shoot and settling time are 0.7×10^{-3} and 0.7×10^{-3} , respectively. Whereas these amounts in designing by the particle swarm algorithm are 0.85×10^{-3} and 1.1×10^{-3} , respectively.

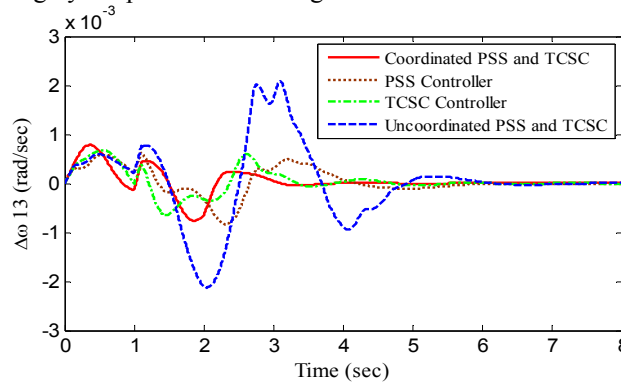


Figure 12. Response of $\Delta\omega_{13}$ for light load condition

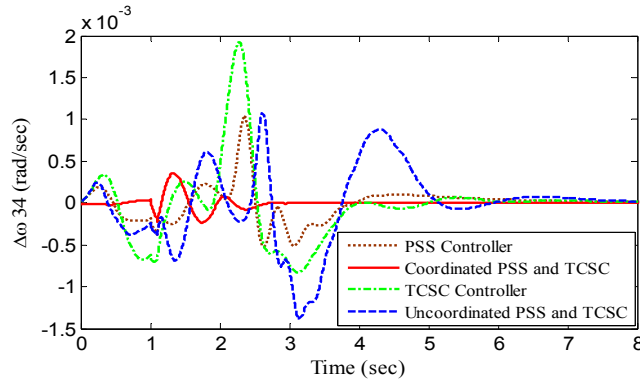


Figure 13. Response of $\Delta\omega_{34}$ for light load condition

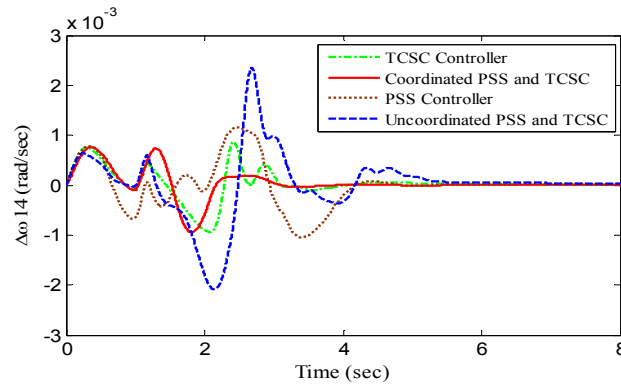


Figure 14. Response of $\Delta\omega_{14}$ for light load condition

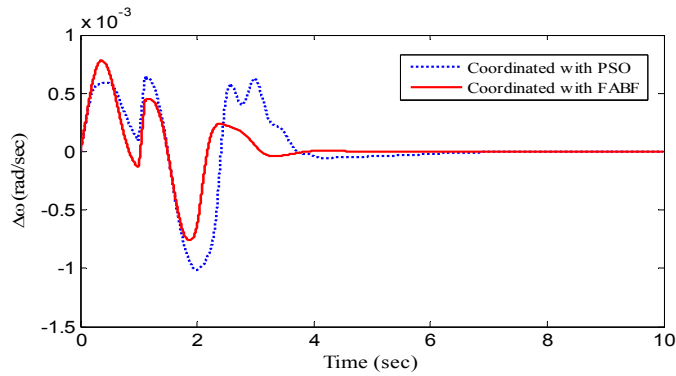


Figure 15. Response of $\Delta\omega_{13}$ for different optimization techniques

D. The heavy loading response results in the 4-machine power system

In this section the output results, resulted from the speed deviation of generators: $\Delta\omega_{13}$, $\Delta\omega_{34}$ and $\Delta\omega_{14}$ by the proposed controllers under nominal loading conditions, were show in figures 16, 17 and 18, respectively. According to these figures, the performance of the proposed controller in the coordination between PSS and TCSC for the reduction of settling time, and thus damping of the power system's oscillations, is clearly observed. In order to further prove the method used in figure 19, the response of $\Delta\omega_{13}$ has been compared using the

two different optimization techniques: FBFA and PSO. According to this figure, the amounts of overshoot, under shoot and settling time are 0.7×10^{-3} and 0.7×10^{-3} , respectively. Whereas these amounts in designing by the particle swarm algorithm are 0.85×10^{-3} and 1.1×10^{-3} , respectively. These results imply the better designing performance of the FABF algorithm for the damping of low frequency oscillations.

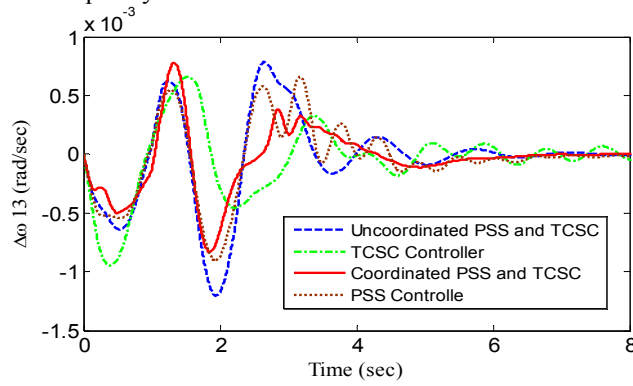


Figure 16. Response of $\Delta\omega_{13}$ for heavy load condition

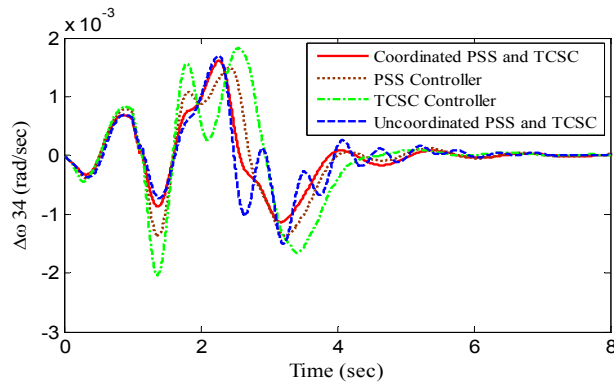


Figure 17. Response of $\Delta\omega_{34}$ for heavy load condition

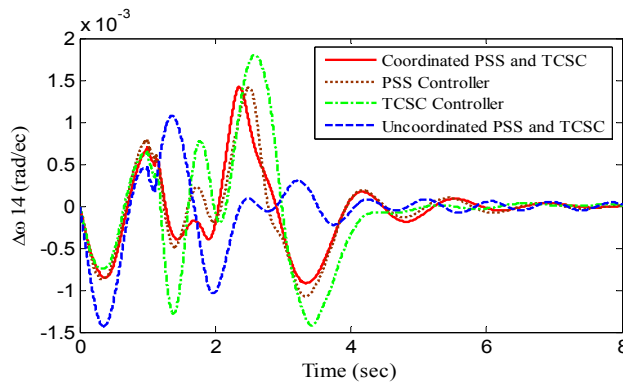
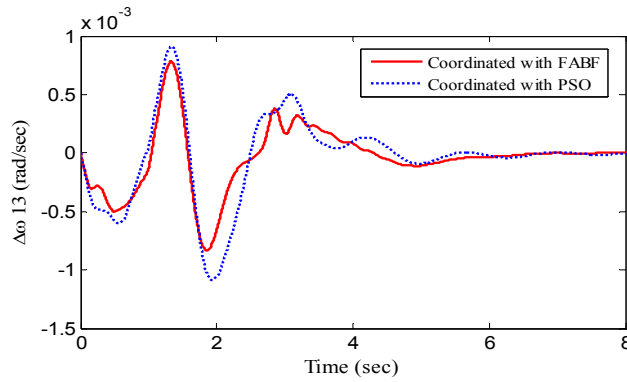
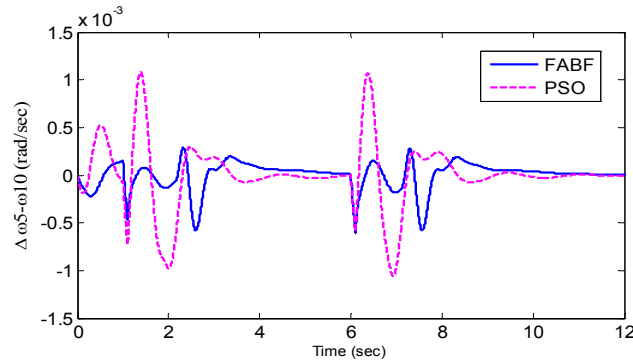


Figure 18. Response of $\Delta\omega_{14}$ for heavy load condition


 Figure 19. Response of $\Delta\omega_{13}$ for different optimization techniques

E. The simulation results of the 10-machine power system

Under nominal performance conditions, two three-phase short-circuit cycles at the times of 1th and 4th second, were placed near bus 20 between the buses (34-20) for 150ms. The speed variations of the generators 4 and 5 compared to generator 10, were shown in figures 20 and 21. According to figure 20, the amounts of overshoot, under shoot and settling time in the design of controllers by the discussed method (FABF) are 0.2×10^{-3} , 0.6×10^{-3} and 4.2s, respectively, whereas these amounts in the design by the PSO method are, 1.12×10^{-3} , 1×10^{-3} and 4.5s, respectively. Moreover, according to the simulation results shown in figure 21, the amounts of overshoot, under shoot and settling time in the design by the proposed method are 0.95×10^{-3} , 0.61×10^{-3} and 4.2s, respectively, whereas in the design by the PSO method, these results were 1.22×10^{-3} , 1.38×10^{-3} and 5.7, respectively. According to the obtained results it can be seen that the proposed method is stronger than the classic method and PSO in stabilizing and reducing the oscillations of the generators. Also since generator 10 has the highest inertia, the speed deviation of it will be lower for the input energy. Thus, all the other generators will have a lower speed oscillation.


 Figure 20. Response of $\Delta\omega_5, \Delta\omega_{10}$ for normal load condition

The way in which the generators' voltages vary, has been given in figures 22 and 23. According to these figures, the amplitude variations of the terminal voltage for them china 4 and 5, compared to generator 10, implies that the installed controllers, damp the error oscillations and voltage stability in less than 2.5 seconds. Also the comparison between the two algorithms FABF and PSO shows that the amount of the damping of low frequency oscillations with the use of FABF algorithm causes the terminal voltage variations amplitude to become zero between the generators.

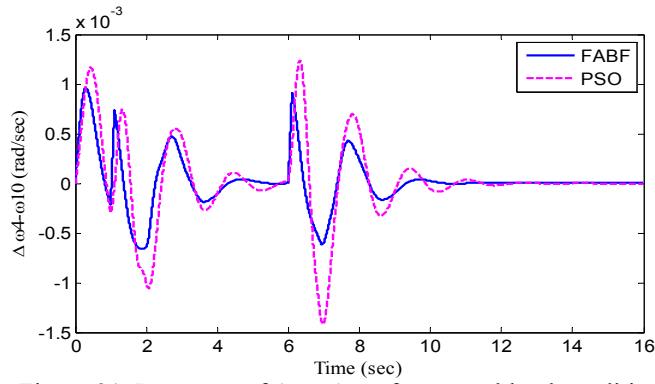


Figure 21. Response of $\Delta\omega_4-\Delta\omega_{10}$ for normal load condition

The way in which the generators' voltages vary, has been given in figures 22 and 23. According to these figures, the amplitude variations of the terminal voltage for thema chines 4 and 5, compared to generator 10, implies that the installed controllers, damp the error oscillations and voltage stability in less than 2.5 seconds. Also the comparison between the two algorithms FABF and PSO shows that the amount of the damping of low frequency oscillations with the use of FABF algorithm causes the terminal voltage variations amplitude to become zero between the generators.

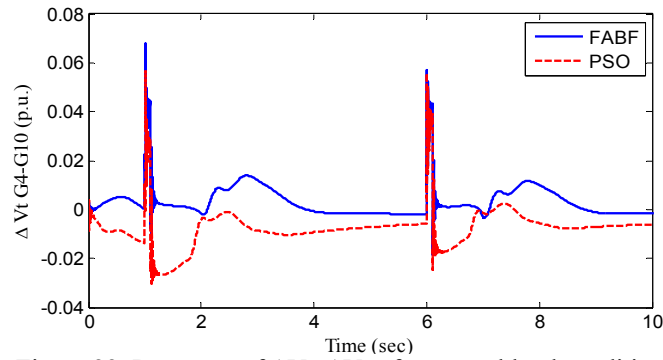


Figure 22. Response of $\Delta V_{t4}-\Delta V_{t10}$ for normal load condition

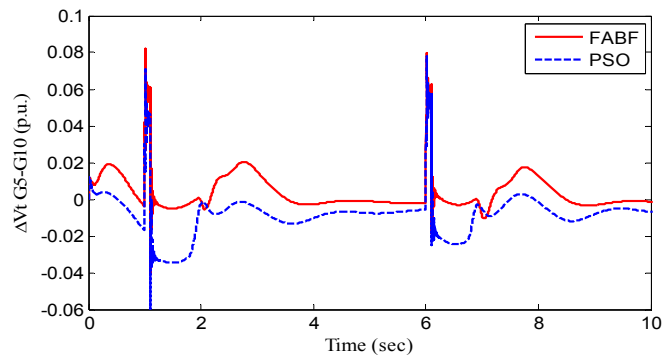


Figure 23. Response of $\Delta V_{t5}-\Delta V_{t10}$ for normal load condition

6. Conclusion

In this paper, the power system stabilizer and TCSC have been designed using FABF algorithm to increase the damping. The simulation results with the use of the proposed method have been coordinated with the results of separate designs of PSS, TCSC and PSS-TCSC, and have been compared using the PSO and FABF algorithms. The capability of the FABF method was proved by investigating the special values in the two inter-area frequency and local frequency modes. The results showed that the fuzzy adaptive bacterial foraging (FABF) gives a better solution than the PSO algorithm for the minimization of the target function. In addition to that, the control system performance gives a more proper response compared to the classic method and PSO, by delaying the variation in signal transmission at the time of error occurrence. For the effectiveness of the proposed method, the simulation results were tested on the kundur 4-machine and the New England 10-machine power systems, and in both systems, the FABF algorithm's results, reduced the low frequency oscillations and thus improved the dynamic response of the tested power systems.

7. References

- [1] Phadke AG, Thorp JS. "Synchronized phasor measurements and their applications", New York: Springer; 2008.
- [2] Yu YN. "Electric power system dynamics", New York: Academic Press; 1983.
- [3] Kundur P. "Power system stability and control", New York: McGraw-Hill; 1994.
- [4] Yang TC. "Applying H_{∞} optimisation method to power system stabilizer design parts 1&2", *Int J Electr Power Energy Syst* 1997;19(1):29–43.
- [5] Kwakernaak H. "Robust control and H_{∞} optimization tutorial", *Automatica* 1993;29(2):255–73.
- [6] J. Sanchez-Gasca, "Coordinated control of two FACTS devices for damping interarea oscillations", *IEEE Trans. Power Syst.*, vol. 13, no.2, pp. 428–434, May 1997.
- [7] R. Mohan, Mathur and R. K. Varma, "Thyristor-Based FACTS Controller for Electrical Transmission System", Piscataway, NJ: IEEE Press/Wiley Interscience, 2002.
- [8] P. He, C. Y. Chung, and Y. Xue, "An eigen structure-based performance index and its application to control design for damping interarea oscillations in power systems", *IEEE Trans. Power Syst.*, vol. 26, no. 4, pp. 2371–2380, Nov. 2011.
- [9] B. Bhattacharyya, S.K.Goswami, V. Kumar Gupta, "Particle Swarm Intelligence based allocation of FACTS controller for the increased load ability of Power system", *IJEEI - Volume 4, Number 4, December 2012*
- [10] Y. C. Chang, R. F. Chang, T. Y. Hsiao, and C. N. Lu, "Transmission system locability enhancement study by ordinal optimization method", *IEEE Trans. Power Syst.*, vol. 26, no. 1, pp. 451–459, Feb. 2011.
- [11] X. Tan, N. Zhang, L. Tong, and Z. Wang, "Fuzzy control of thyristor controlled series compensator in power system transients", *Sets Syst.*, vol. 110, pp. 429–436, 2000.
- [12] X. Lei, E. N. Lerch, and D. Povh, "Optimization and coordination of damping controls for improving system dynamic performance", *IEEE Trans. Power Syst.*, vol. 16, no. 3, pp. 473–480, Aug. 2001.
- [13] Li BH, Wu QH, Turner DR, Wang PY, X Zhou X. "Modeling of TCSC dynamics for control and analysis of power system stability", *Int J Electr Power Energy Syst* 2000;22(1):43–9.
- [14] M. Kashki, M. A. Abido, Y. L. Abdel-Magid. "Pole placement approach for robust optimum design of PSS and TCSC-based stabilizers using reinforcement learning automata", *Springer, Electrical Engineering*, March 2010, Volume 91, Issue 7, pp 383-394.
- [15] Simoes, A. M., Savelli, D. C., Pellanda, P. C., Martins, N., Apkarian, P., "Robust Design of a TCSC Oscillation Damping Controller in a Weak 500-kV Interconnection

- Considering Multiple Power Flow Scenarios and External Disturbances”, *IEEE Trans. On Power Systems*, pp.226, 2009.
- [16] Johansson, N., Angquist, L., Nee, H. P., “An Adaptive Controller for Power System Stability Improvement and Power Flow Control by Means of a Thyristor Switched Series Capacitor”, *IEEE Trans. On Power Systems*, pp.381, 2010.
- [17] Chen, R. R. Mohler, L. K. Chen, “Synthesis of Neural Controller Applied to Flexible AC Transmission Systems”, *IEEE Trans. On Circuits and Systems I: Fundamental Theory and Applications*, Vol. 47, Issue 3, pp. 376-388, 2000.
- [18] S.Hameed, “Power System Stability Enhancement Using Reduced Rule Base Self-Tuning Fuzzy PI Controller for TCSC”, 2010 IEEE PES, pp.1, 2010.
- [19] Dai Wenjin Chen Xiangjie Lin Qingsheng, “Fuzzy Self-Adaptive PID Control Based on BP Neural Network for TCSC”, *International Conference on Intelligent Human-Machine Systems and Cybernetics*, pp.178, 2009.
- [20] M-R. Banaei, B. Mohammadzadeh, R.RezamAhrabi, “Damping of Low Frequency Electro-Mechanical Oscillations Using UPFC Based on Cuckoo Optimization Algorithm”, *IJEEI*, Volume 6, Number 4, December 2014.
- [21] Wagh, S. R. Kamath, A. K. Singh, N. M., “Nonlinear Model Based Control with Prior Knowledge Based Learning”, *7th Asian Control Conference*, pp. 1576, 2009.
- [22] Wagh, S. R. Kamath, A.K. Singh, N. M., “A Nonlinear TCSC Controller Based on Control Lyapunov Function and Receding Horizon Strategy for Power System Transient Stability Improvement”, *IEEE International Conference on Control and Automation, ICCA*, pp. 813, 2009.
- [23] R. Narne, P-Ch. Panda, “Coordinated Design of PSS with Multiple FACTS Controllers using Advanced Adaptive PSO”, *IJEEI*, Volume 5, Number 3, September 2013.
- [24] Abido MA. “Pole placement technique for PSS and TCSC based stabilizer design using simulated annealing”, *Int J Electric Power Energy Syst* 2000;22(8):543–54.
- [25] Shayeghi H, Safari A, Shayanfar HA. “PSS and TCSC damping controller coordinated design using PSO in multimachine power system”. *Int J Energy Convers Manage* 2010;51(12):2930–7.
- [26] E.S. Ali , S.M. Abd-Elazim. “Coordinated design of PSSs and TCSC via bacterial swarm optimization algorithm in a multimachine power system”, *Int J Electrical Power and Energy Syst* 36 (2012) 84–92.
- [27] K.M. Passino, “Biomimicry of bacterial foraging for distributed optimization and control”, *IEEE Control Systems Magazine* (2002) 52–67.
- [28] ChVenkaiah, D.M. Vinod Kumar. “Fuzzy adaptive bacterial foraging congestion management using sensitivity based optimal active power re-scheduling of generators”, *Int. J Applied Soft Computing* 11 (2011) 4921–4930.
- [29] Faisal SF, Rahim AHMA, Bakhshwain JM. “Robust STATCOM controller for a multi-machine power system using particle swarm optimization and looshaping”, *Int J Electr. Comput. Syst. Eng* 2007;1(1):64–70.
- [30] Mishra, S., Tripathy, M., Nanda, J. “Multi-machine power system stabilizers designed by rule based bacteria foraging”, *Electr. Power Syst. Res.*, 2006, 77, pp. 1595–1607.
- [31] M. Tripathy, S. Mishra: “Interval type-2-based thyristor controlled series capacitor to improve power system stability”, *IET Gener. Transm. Distrib.*, 2011, Vol. 5, Iss. 2, pp. 209–222.